Structural Steels Microstructural Homogeneity Effect on Fatigue Performance in Air and Hydrogen Environments

Authors

Douglas Stalheim (left)
President, DGS Metallurgical Solutions Inc., Vancouver, Wash., USA
dgstalheim@comcast.net

Andrew Slifka
National Institute of Standards and Technology, Boulder, Colo., USA
andrew.slifka@nist.gov

Enrico Lucon
National Institute of Standards and Technology, Boulder, Colo., USA
enrico.lucon@nist.gov

Pello Uranga (right)
Associate Director of Materials and Manufacturing Division, CEIT, Member of Basque Research & Technology Alliance (BRTA), and University of Navarra, Basque Country, Spain
puranga@ceit.es

Dong-Hoon Kang
Hyundai Steel Technical Research Center, Dangjin, Chungnam, Korea
dhkang12@hyundai-steel.com

Strength and ductility properties of structural steels for a given microstructure are driven by the average ferrite grain/packet size and by the homogeneity of that ferrite grain/packet size in the final product. Fatigue performance in air for applications of wind towers, bridges, or high-rise buildings and in high-pressure gaseous hydrogen for various pipeline systems is critical to the end-use design. To evaluate the effect of cross-sectional ferrite grain size and homogeneity on fatigue performance, samples with differences in average ferrite grain size and homogeneity were produced and tested in both air and high-pressure gaseous hydrogen.

Fatigue performance in air for applications of wind towers, bridges, or high-rise buildings and in high-pressure gaseous hydrogen for various pipeline systems is critical to the end-use design. Most codes that provide for proper design of structures that are susceptible to fatigue, such as the ASME B31.12 code for Hydrogen Piping and Pipelines, base the designs on the strength of the materials.[1] However, strength is not the only consideration in the fatigue resistance of a material, particularly for structural steels, and many structural applications result in loading conditions where fatigue resistance is more important than strength. The mechanical properties of a steel come from microstructure and chemistry, and microstructure is developed from processing of that chemistry. Strength and ductility properties of structural steels for a given microstructure are primarily driven by the average ferrite grain/packet size and by the homogeneity of that ferrite grain/packet size in the final product. Therefore, fatigue resistance of steels is developed from processing and is intimately tied to cross-sectional microstructure.[2–5] To evaluate the effect of cross-sectional ferrite grain size and homogeneity on fatigue performance, samples with differences in average ferrite grain size and homogeneity were produced and tested in both air and high-pressure gaseous hydrogen.

In the past 10 years, the National Institute of Standards and Technology (NIST), Sandia, Powertech Laboratory (Canada) and various other U.S. national laboratories have performed fracture and fatigue testing in air and hydrogen of various structural steel microstructures. Many of these microstructures were related to various API grade pipeline steels. NIST has focused on fatigue testing utilizing a uniquely developed multi-specimen fatigue testing device with capability for both air and high-pressure gaseous hydrogen atmospheres. This device significantly increases the productivity of the fatigue test.[6] Both NIST and Sandia National Laboratories have fracture and fatigue tested a produced API X60 hydrogen-induced cracking (HIC) sour service plate–grade microstructure consisting of a low-carbon (0.03%) and higher niobium content (0.085%) that, when processed, developed a predominately pure microstructure of polygonal ferrite. This microstructure was identified as "Alloy D" in the fracture and fatigue testing done in high-pressure gaseous hydrogen. This microstructure has performed well in both 800 and

This article is available online at AIST.org for 30 days following publication.

Figure 1

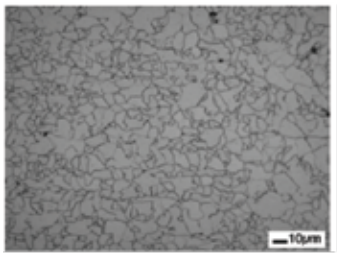

Optical of Alloy D, predominately polygonal ferrite

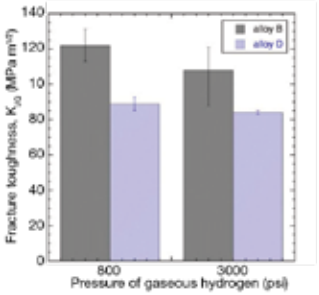

Alloy D fracture toughness at 800/3,000 psi hydrogen pressure. Note the stability.

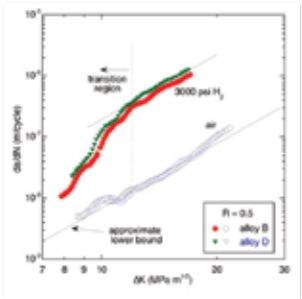

Alloy D fatigue testing in air and 3,000 psi hydrogen pressure

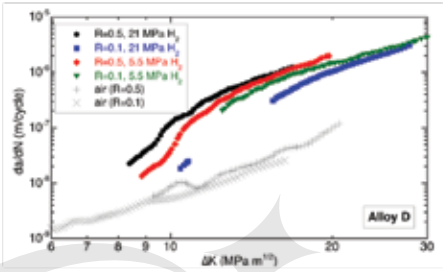

Alloy D fatigue testing in air, 800 and 3,000 psi hydrogen pressure

Example of original Alloy D fracture/fatigue performance in high-pressure gaseous hydrogen, 800 and 3,000 psi.

3,000 psi hydrogen pressure fracture and fatigue testing (Fig. 1).[7–11]

While this alloy/processing designed microstructure has performed well overall in fatigue testing, a question raised was how the fatigue performance in air or high-pressure gaseous pressure would be affected for this alloy/microstructure design if the cross-sectional final ferrite grain size homogeneity varied.

Material Design

The only way to single out and design the desired cross-sectional microstructure/grain size homogeneity was to produce an optimized and non-optimized metallurgical processing in the pilot laboratory rolling mill. Since final ferrite grain size and homogeneity is controlled by the development of the various austenite recrystallization behaviors, Type I Static Recrystallization, Type II No Recrystallization and Type III Partial Recrystallization behaviors during hot deformation.[12] The optimized processing design, Alloy D1O (Optimized), was done utilizing an optimum percentage of total Type I Static Recrystallization (50–60% is critical to cross-sectional homogeneity) behavior and Type II No-recrystallization (56%) behavior for the niobium content and starting vs. final thickness of the laboratory plates. The non-optimized processing design, Alloy D2NO (Non-optimized), was

Table 1

Alloy Design and Mechanical Properties vs. Actual Lab Melt and Mechanical Properties

	C	Mn	Si	Cr	Cu	Ni	Nb	Yield strength, MPa (0.2% offset)	Tensile strength, Mpa	El
Original Alloy D	0.030	1.140	0.180	0.160	0.240	0.140	0.084	435	486	—
Alloy D1O	0.030	1.200	0.160	0.160	0.260	0.160	0.088	520	585	36.500
Alloy D2NO	0.030	1.160	0.150	0.150	0.260	0.150	0.084	482	572	31.100

Table 2

Roughing/Finishing/Cooling Strategy Design vs. Actual Lab Achieved

	Reheat °C	RM FRT °C	RM total reduction %	Hold thickness mm	FM start °C	FM FRT °C	FM total % reduction	Start cool °C	FCT °C	CR °C
Design	1,180	>1,050	D1O–55, D2NO–35	D1O–45, D2NO–65	D1O–880, D2NO–1,000	D1O–820–840, D2NO–850–880	D1O–56, D2NO–69	D1O–>800, D2NO–>800	D1O–650, D2NO–700	3–5
Alloy D1O	1,180	1,132	55	45	864	843	56	822	648	8.7
Alloy D2NO	1,180	1,115	35	65	1,004	886	69	856	715	8.8

Figure 2

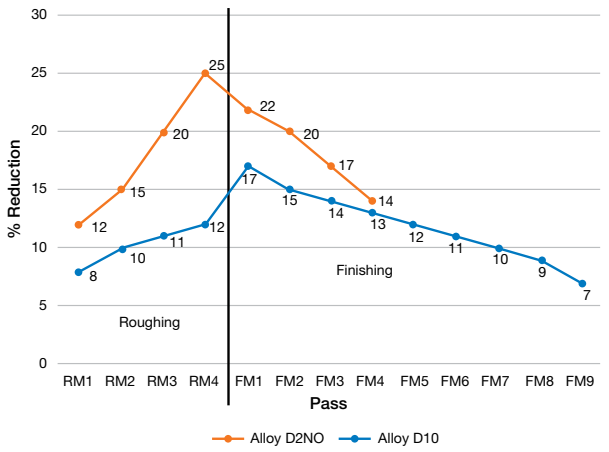

Per-pass reduction schedule.

Figure 3

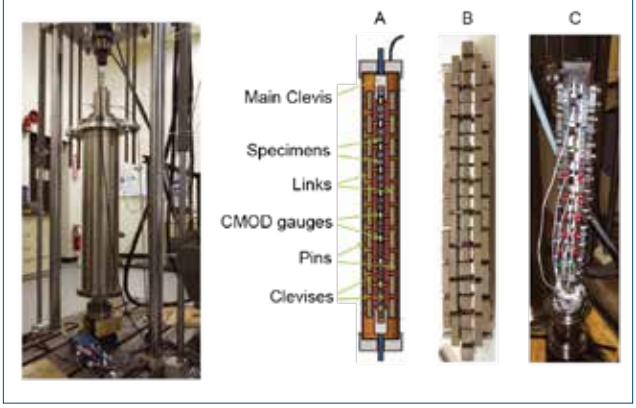

National Institute of Standards and Technology (NIST) test vessel for pressurized hydrogen gas.

done utilizing a non-optimum Type I Static Recrystallization (35%, to create a heterogeneous cross-sectional final ferrite grain size) behavior and Type II No-recrystallization/Type III Partial Recrystallization (65%, Type III Partial Recrystallization further aggravates the heterogeneity of the cross-sectional grain size) behavior. The optimized vs. non-optimized conditions for the austenite recrystallization behavior and final cross-sectional austenite homogeneity were produced by varying the per-pass reduction schedules, holding thickness and start finishing temperatures relative to the Nb content. The laboratory ingot size was 100 x 170 x 300 mm and was rolled into a 20 x 180 x 1,300 mm final plate dimension for the investigation. In total, eight ingots/plates, four optimized and four non-optimized were produced. The original "Alloy D" design vs. actual achieved, rolling strategy design vs. actual achieved and original mechanical properties for "Alloy D" vs. the material for the project, Alloy D1O and Alloy D2NO, are shown in Tables 1 and 2. Per-pass reduction schedules for Alloy D1O and Alloy D2NO are shown in Fig. 2.

Figure 4

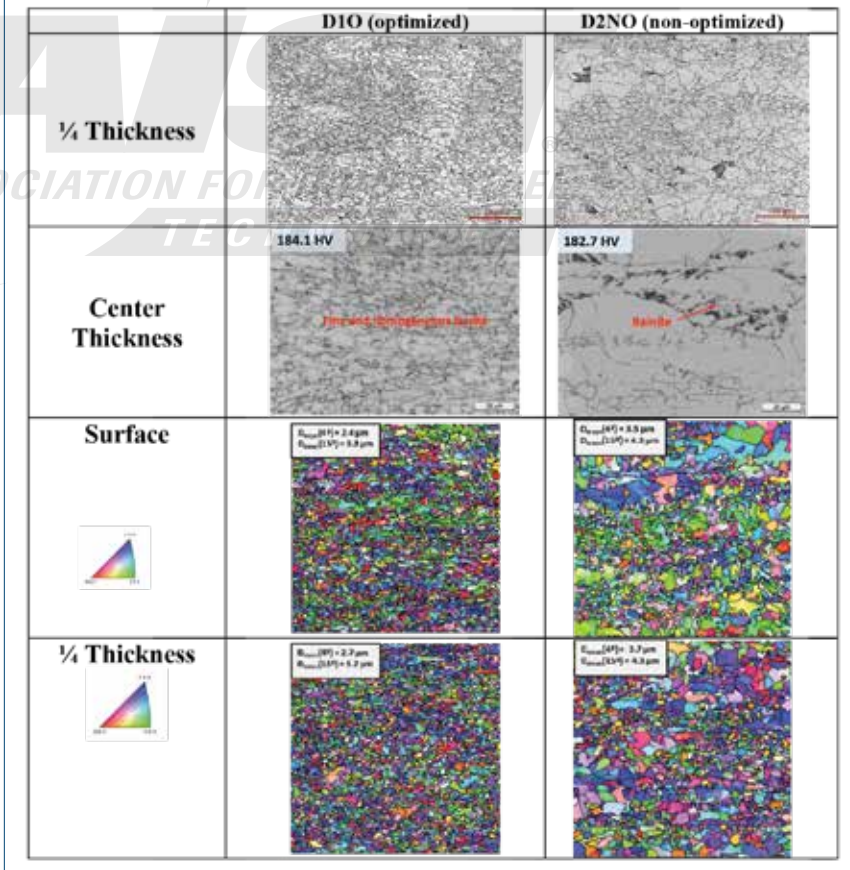

Detailed microstructural characterization showing obvious differences in cross-sectional final ferrite grain size homogeneity of low-angle grain boundary (LAGB) and high-angle grain boundary (HAGB). HAGB are critical to ductility properties such as fatigue.

Figure 4 (cont'd)

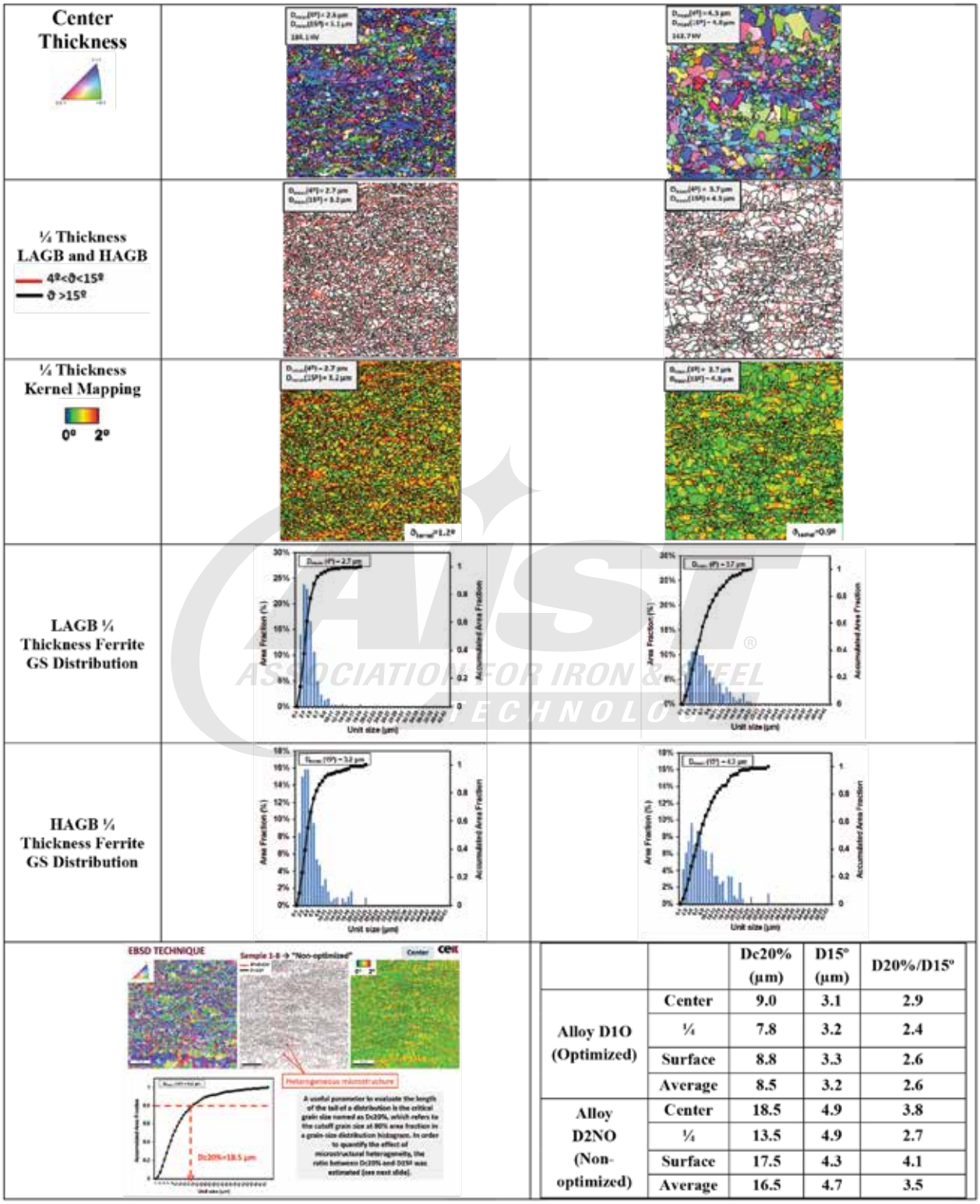

		Dc20% (µm)	D15º (µm)	D20%/D15º
Alloy D1O (Optimized)	Center	9.0	3.1	2.9
	¼	7.8	3.2	2.4
	Surface	8.8	3.3	2.6
	Average	8.5	3.2	2.6
Alloy D2NO (Non-optimized)	Center	18.5	4.9	3.8
	¼	13.5	4.9	2.7
	Surface	17.5	4.3	4.1
	Average	16.5	4.7	3.5

Detailed microstructural characterization showing obvious differences in cross-sectional final ferrite grain size homogeneity of LAGB and HAGB. HAGB are critical to ductility properties such as fatigue.

Fatigue testing was performed in the NIST uniquely designed multi-sample fatigue testing pressure vessel (Fig. 3).

Fatigue testing has been done to date in air and now in high-pressure gaseous hydrogen (21 MPa, 3,000 psi). Fatigue testing has been done in accordance with ASTM E647 at load ratios, R, of 0.1 and 0.5.[13] The loading frequency has been 1 Hz, which gives time for hydrogen to diffuse to the crack tip yet is a rate which is fast enough to perform the tests in a reasonable amount of time. The tests have been run in load control, and each specimen has had a crack mouth opening displacement (CMOD) gauge such that crack growth can be determined from compliance. Compact tension (CT) specimens have been machined from the plates of both the D1O and D2NO materials, with the crack oriented in the rolling direction for half of the specimens and perpendicular to the rolling direction for the other half of the specimens. The test chamber has an actuator rod that extends from inside the chamber to outside of the chamber. There are three seals along the length of the actuator rod, and those seals impart load to the actuator rod. Because that load is sometimes inconsistent, an internal load cell is used within the chamber such that no compensation for friction of the seals is required. The specimens have length W = 45 mm and thickness B = 19 mm.

Results and Discussion

Microstructural Characterization — In comparing the two steels, it is important to do a detailed microstructural characterization of the cross-sectional microstructure for comparison to the fatigue results. This "optimized" and "non-optimized" laboratory rolling strategy resulted in distinct differences in the cross-sectional final ferrite grain size and homogeneity. Since strength properties are significantly controlled by low-angle grain boundaries (LAGB $4^{o}<\vartheta<15^{o}$, D4°) and ductility properties, such as toughness and fatigue, are significantly controlled by high-angle grain boundaries (HAGB, $\vartheta > 15^{o}$, D15°), microstructural characterization of the laboratory-produced plates of both low-angle grain boundaries and high-angle grain boundaries was performed. The goal of creating similar microstructures in the two laboratory plates with distinctly different cross-sectional final ferrite grain size/homogeneity was realized (Fig. 4).[14,15] The microstructure in both the optimized and non-optimized plates was predominately polygonal ferrite with a very small amount of pearlite/bainite seen in the non-optimized plates due to the coarse austenite grain size. The optimized plates had an average cross-sectional HAGB ferrite grain size of 3.2 µm with 20% of the cross-sectional average HAGB > 8.5 µm. The non-optimized plates had an average cross-sectional HAGB ferrite grain size of 4.5 µm with 20% of the cross-sectional average HAGB > 16.5 µm. For optimum ductility properties, average HAGB (finer is better) and the population of larger HAGB representing more than 20% of the accumulated area fraction (finer is better) is the target goal. Kernel mapping shows a slightly higher dislocation density in the Alloy D1O (Optimized).

MicroSim® Austenite Evolution Modeling Results — In addition, modeling of austenite grain size evolution utilizing MicroSim PM V3 has been done utilizing the processing parameters from the laboratory rolling for comparison with the final observed polygonal microstructure. MicroSim modeling of the austenite evolution at the end of the roughing phase and in the finishing phase show that while the averages are relatively similar, there is a large difference in the largest austenite grain (D_{Max}), 90% of the austenite grains below value (DC 0.1) and ZD (cross-sectional homogeneity factor, smaller is more homogenous). In addition, the final austenite grain size distribution prior to accelerated water cooling (ACC) between the optimized and non-optimized rolling shows an obvious difference (Fig. 5).

Charpy Test Results — As a precursor to fatigue testing, transverse Charpy impact testing of the two steels was performed at NIST with temperatures ranging from –196°C to 21°C (room temperature). Testing was done in accordance with ASTM E 23.[16] The parameters measured were absorbed energy, KV, and lateral expansion, LE. Ductile-to-brittle transition temperatures (DBTT) were obtained from curves of KV and LE as a function of temperature, shown in Fig. 6. Upper-shelf energy (USE) is calculated from data in Fig. 6. There is no difference in USE between the steels, but the non-optimized steel is 25°C more brittle than the optimized steel. The noted USE differences (no difference) are as expected for this very low carbon, lower Mn, low S, inclusion-controlled polygonal ferrite microstructure. The DBTT (25°C difference) would be expected due to the differences in HAGB average and heterogeneity through the cross-section.

Fatigue Test Results — Fatigue crack growth rate (FCGR) testing in air and 21 MPa (3,000 psi) pressure gaseous hydrogen, for both the optimized and non-optimized steels, has been completed. CT specimens with W = 45 mm and B = 19 mm have been machined from the plates. Half of the specimens have T-L orientation and half have L-T orientation, where the first letter designates the loading direction and the second is the direction of crack growth. L is the longitudinal, or plate rolling direction, and T is the direction

Figure 5

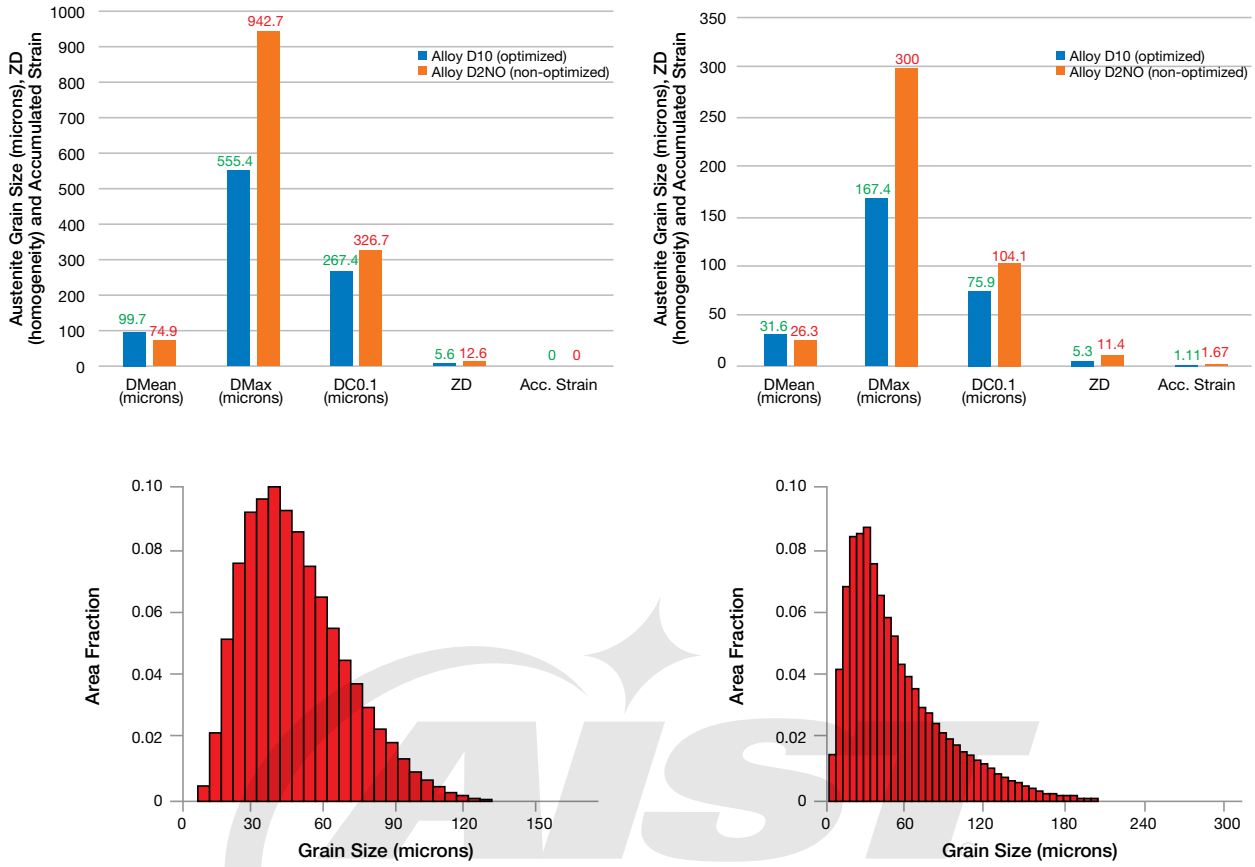

Roughing and Finishing MicroSim® modeling of austenite evolution and final austenite grain size distribution.

transverse to the rolling direction. All specimens have cracks extending through the thickness of the plates.

Fatigue Testing in Air Results — Fatigue testing in air has been completed. Key observations of the data are as follows (Fig. 7):

1. Optimized rolling (finer, more homogenous cross-sectional grain size) has significantly higher fracture toughness capability (2X-7X), as seen in pre-cracking.
2. Both optimized and non-optimized have a narrow distribution in crack growth rate performance at low ΔK (stress intensity factor), however the non-optimized crack growth rate is higher than the optimized crack growth rate.

Figure 6

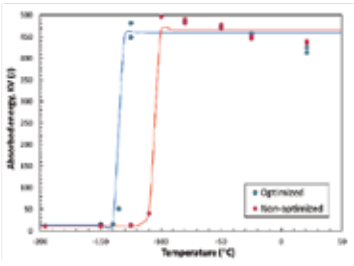

(a)

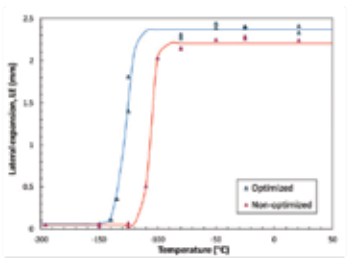

(b)

Material	$DBTT_{KV}$	USE	$DBTT_{LE}$
Condition	(°C)	(J)	(°C)
Optimized	–133	459	–128
Non-optimized	–108	466	–107

(c)

Transverse Charpy performance: absorbed energy as a function of temperature for both steels (a), lateral expansion as a function of temperature for both steels (b) and summary of Charpy testing (c).

Figure 7

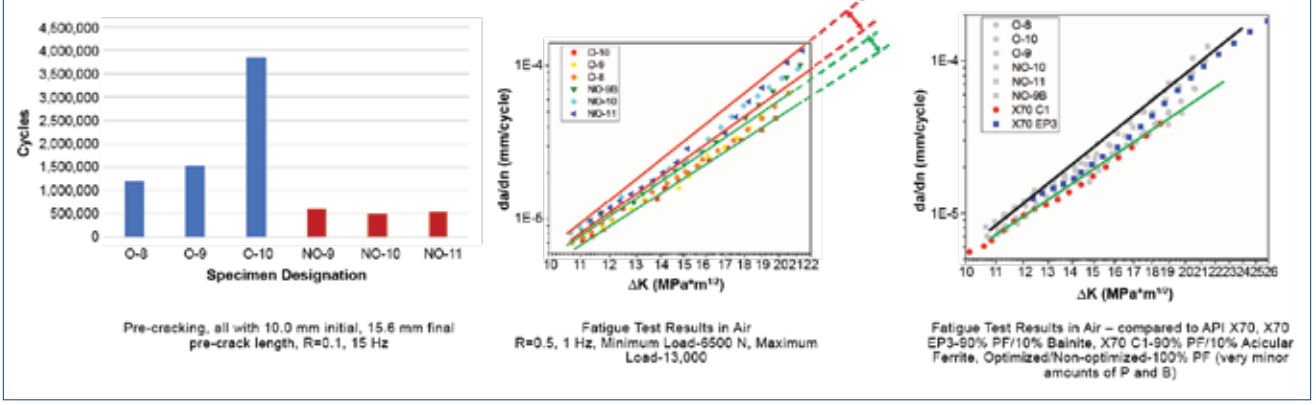

Fatigue test results in air.

3. As the stress intensity factor increases, the non-optimized crack growth rate distribution starts to diverge while the optimized continues to maintain a tighter crack growth rate distribution.
4. The non-optimized crack growth rate is slightly higher than a production produced higher-strength PF/B X70. This suggests that cross-sectional grain size/homogeneity has a more dominate effect on fatigue than strength, a small volume fraction of bainite or inclusions.
5. The optimized crack growth rate is like that of a production produced higher-strength PF/AF X70. This suggests that cross-sectional grain size/homogeneity can have a similar effect to producing a small volume fraction of acicular ferrite microstructure.

Fatigue Testing in 21 MPa (3000 psi) Gaseous Hydrogen Results — Fatigue testing in gaseous hydrogen at 21 MPa (3,000 psi) has been completed. Key observations of the data are as follows (Fig. 8):

1. Again, as seen in the air testing, the fracture toughness of the optimized steel was significantly better than the non-optimized steel. The optimized specimens took twice as many cycles, on average, to generate the same length pre-crack length as the non-optimized specimens under the same loading conditions.
2. The non-optimized steels show very consistent fatigue crack rate growth performance from all three specimens. The optimized steels show much improved resistance to crack growth in hydrogen. However, one of those specimens shows higher crack growth rate than the other two, despite similarities in

Figure 8

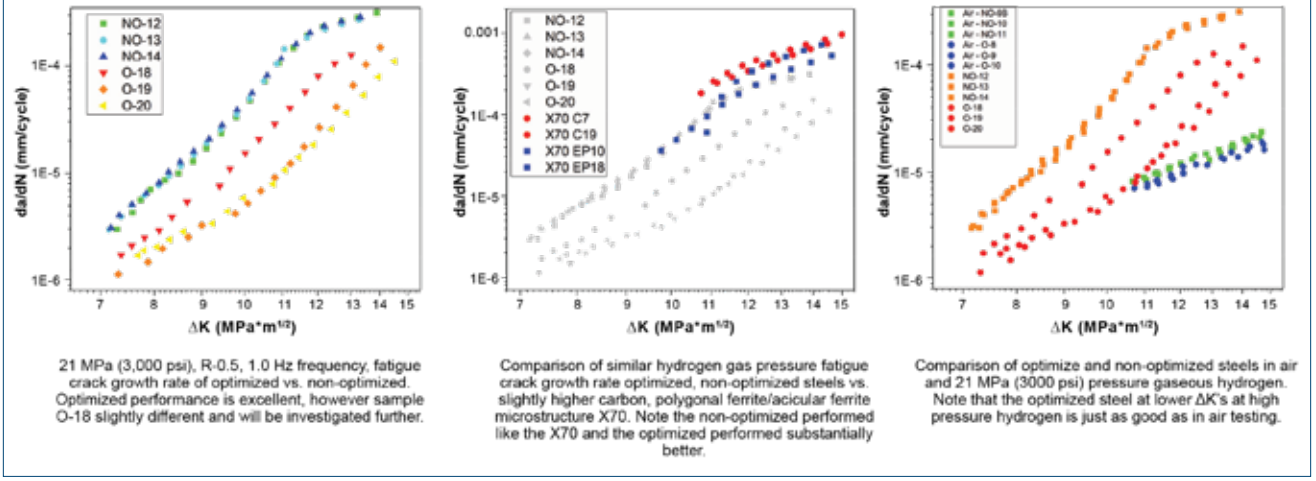

Fatigue results of optimized and non-optimized steels 21 MPa (3,000 psi) high-pressure gaseous hydrogen.

the pre-crack size and crack shape and cycles to pre-crack to the same initial crack length (15.6 mm). This will be investigated further to determine cause.

3. When compared at similar hydrogen gas pressure, the fatigue crack growth rate of the optimized steel vs. two slightly higher carbon and different microstructure, polygonal ferrite/acicular ferrite slightly coarser (average cross-sectional ferrite grain size in the 10–15 µm range) and less homogenous production X70 performed substantially better, while the non-optimized steels vs. the same two X70 steels performed the same. This shows again how cross-sectional grain size can affect fatigue performance.
4. The optimized and non-optimized (both air and hydrogen) data shows how good the optimized alloy is at 21 MPa (3,000 psi) gaseous hydrogen pressure. The optimized steel at 21 MPa (3,000 psi) pressure at low ΔKs is as good or better than in air testing. Again, this illustrates the importance of cross-sectional grain size homogeneity of ductility properties such as fatigue.

Additional fatigue testing in gaseous hydrogen will continue looking at a comparison of specific optimized rolled samples with additional microstructural characterization to further document detailed differences and overall consistency. In addition, lower hydrogen pressures of 5.5 MPa (800 psi) will be explored.

Conclusion

The following conclusions can be made:

1. A predominately polygonal ferrite microstructure with good cleanliness and no microstructural banding but with varying cross-sectional ferrite grain size/distribution has been successfully produced in the laboratory.
2. This will allow for a proper evaluation of the effect the cross-sectional ferrite grain size/distribution will have on ductility properties, such as fatigue performance for a given microstructure in air and high-pressure gaseous hydrogen.
3. Charpy impact test results show that there is no difference between the use of the two steels as would be expected from the low-carbon, low-sulfur clean steel polygonal ferrite microstructure produced, but the non-optimized steel, while of the same cleanliness quality, is 25°C more brittle than the optimized steel as would be expected due to the difference in cross-sectional ferrite grain size/heterogeneity.
4. Pre-cracking shows that the optimized steel has significantly higher fracture toughness than the non-optimized steel.
5. Fatigue testing in air showed the following:
   - The non-optimized steel shows more divergence in crack growth rate with increasing ΔK than that of the optimized steel.
   - The lower-strength non-optimized steel has higher crack growth rate than that of production produced higher-strength X70 with various bainitic microstructural phases.
   - The lower-strength optimized steel has a lower crack growth rate of a production produced X70 with 10% bainite and similar crack growth rate to that of a production produced X70 with 10% acicular ferrite microstructure.
6. Fatigue testing in high-pressure gaseous hydrogen (21 MPa, 3,000 psi) showed the following:
   - The optimized steels show much improved resistance to crack growth in hydrogen than that of the non-optimized steel.
   - When compared at similar hydrogen gas pressure the fatigue crack growth rate of the optimized steel vs. two higher-carbon different microstructure, polygonal ferrite/acicular ferrite slightly coarser (average cross-sectional ferrite grain size in the 10–15 µm range) and less homogenous production X70 performed substantially better, while the non-optimized steels vs. the same two X70 steels performed the same.
   - The optimized and non-optimized (both air and hydrogen) data shows how good the optimized alloy is at 21 MPa (3,000 psi) gaseous hydrogen pressure. The optimized steel at 21 MPa (3,000 psi) pressure at low ΔKs is as good or better than in air.
7. It has been shown in both air and high-pressure gaseous hydrogen the importance that the cross-sectional grain size/homogeneity has in fatigue crack growth rate for the same alloy design, microstructure and strength level.

This paper is a continuation of a series of papers, with several more papers on the subject as additional fatigue data is generated from the samples produced

at different hydrogen pressures. This study on the effect on cross-sectional grain size homogeneity may be expanded to higher carbon structural steels with various microstructural phases (i.e., ferrite/pearlite) along with a level of cleanliness and precipitation strengthening mechanisms in the future.

Acknowledgments

The authors wish to thank H2C in Korea for assistance in coordination of the project in Korea, Hyundai Steel Corp. for their cooperation in producing the laboratory samples, and CBMM for providing funding for microstructural characterizations.

References

1. ASME B31.12-2014, Hydrogen Piping and Pipelines, American Society of Mechanical Engineers, New York, N.Y., USA, 2014.
2. J. Lu, D. Ivey, H. Henein, J. Wiskel and O. Omotoso, "Microstructure Characterization and Strengthening Mechanisms of Microalloyed Steels," *Proceedings of 2008 ASME International Pipeline Conference,* Calgary, Alta., Canada, September 2008.
3. R. Barbosa, J.M. Rodríguez-Ibabe, D. Stalheim and M. Rebellato, "Alloy Cost Optimization Through Proper Metallurgical Development of Strength and Ductility Properties in Structural Steels," *AISTech 2018 Conference Proceedings,* 2018.
4. D. Stalheim, "Generation of Stable Optimized Through-Thickness Mechanical Properties in Wide Heavy-Gauge Structural Steel Plate," *AISTech 2018 Conference Proceedings,* 2018.
5. N. Isasti, D. Jorge-Badiola, M.L. Taheri and P. Uranga, "Microstructural Features Controlling Mechanical Properties in Nb-Mo Microalloyed Steels Part II: Impact Toughness," *Metallurgical. Material Transaction A,* Vol. 45A, 2014, pp. 4972–4982.
6. E.S. Drexler, J.D. McColskey and A.J. Slifka et al., *Apparatus for Accelerating Measurements of Environmentally Assisted Fatigue Crack Growth at Low Frequency,* Society for Experimental Mechanisms, 2014.
7. D. Stalheim, "Materials Solutions for Hydrogen Delivery in Pipelines," 2011 US DOE Hydrogen Program Annual Merit Review and Peer Evaluation Meeting, Arlington, Va., USA, 2011.
8. D. Stalheim, "Final Report on Fracture Toughness Testing in Gaseous Hydrogen – Phase 1, Internal report to ASME ST-LLC," January 2011.
9. D. Stalheim, T. Boggess, C. San Marchi, B. Somerday, M. Govindarajan and P. Sofronis et al., "Microstructure and Mechanical Property Performance of Commercial Grade API Pipeline Steels in High Pressure Gaseous Hydrogen," *Proceedings ASME 8th International Pipeline Conference,* Calgary, Alta., Canada, 2010.
10. D. Stalheim, T. Boggess and D. Bromley et al., "Continued Microstructure and Mechanical Property Performance Evaluation of Commercial Grade API Pipeline Steels in High-Pressure Gaseous Hydrogen," *Proceedings ASME 9th International Pipeline Conference,* Calgary, Alta., Canada, 2012.
11. C. San Marchi, B. Somerday, K. Nibur and D. Stalheim, "Fracture and Fatigue of Commercial Grade API Pipeline Steels in Gaseous Hydrogen," *Proceedings of ASME 2010 Pressure Vessels and Piping Division/K-PVP Conference,* Bellevue, Wash., USA, 2010.
12. D. Stalheim, "Understanding Recrystallization Behaviors for Optimization of Stable Mechanical Properties and Improved Yield," *Proceedings 2015 SEAISI Conference and Exhibition,* Manila, Philippines, May 2015.
13. ASTM Standard E 647-11, Test Method for Measurement of Fatigue Crack Growth Rates, 2011, ASTM International.
14. D.H. Kang, "HSC RD Lab Test Results Related to H_2 Infrastructure Development," Hyundai Steel Corp., Internal Project Correspondence, January 2019.
15. P. Uranga, J.M. Rodríguez-Ibabe, N. Isasiti and X. Azpeitia, "High-Pressure Gaseous Hydrogen Pipe," CEIT, Internal Project Correspondence, February 2019.
16. ASTM Standard E 23-18, Standard Test Methods for Notched Bar Impact Testing of Metallic Materials, ASTM International, 2018. ✦

This paper was published in the AISTech 2020 Conference Proceedings. AIST members can access the AISTech 2020 Conference Proceedings in the AIST Digital Library at digital.library.aist.org.

Did You Know?

Refractories Manufacturer Sees Successful Trial of Phenol-Free Brick

South Korean refractories maker Wonjin Worldwide is developing a phenol-free refractory brick, which already has been successfully trialed as a ladle liner at a Korean electric arc furnace (EAF) mill.

According to the manufacturer, its phenol-free brick solves a problem associated with the phenol-resin-bonded bricks commonly used as ladle liners: it doesn't emit volatile organic compounds when heated.

"The most common ladle refractory lining is phenol-resin-bonded brick with magnesia, carbon and alumina components. Despite that resin-bonded bricks are dried to around 250°C to remove volatiles, remaining phenol substances still emit a small amount of various chemical substances during pre-heating, creating significant odors.

"This new phenol-free technology has a significant advantage over the existing technology as it doesn't emit any gases significantly other than carbon dioxide. It also doesn't require any further treatment, whereas the existing improved resin-bonded brick technology requires further heat treatment at higher temperature, an inadequate solution due to the higher cost as well as remaining resin components deep inside of bricks," the company said.

Wonjin Worldwide said it worked with South Korea's largest EAF facility over the last three years to develop the brick, a solution to worker complaints about odors, especially from overhead crane operators.

"We hope this (product) will spread fast to other steel plants and the whole industry, and we expect to become a new industry standard very soon," the company said.